PHYSICAL REVIEW B VOLUME 50, NUMBER 12 15 SEPTEMBER 1994-II

Single-electron tunneling effects in granular metal films

E. Bar-Sadeh and Y. Goldstein
Racah Institute of Physics, The Hebrew University, Jerusalem 91904, Israel

C. Zhang, H. Deng, and B. Abeles
Exxon Research and Engineering, Annandale, New Jersey 08801

O. Millo*
Racah Institute of Physics, The Hebrew University, Jerusalem 91904, Israel
(Received 4 May 1994; revised manuscript received 4 August 1994)

Cryogenic scanning tunneling microscopy is used to study local electrical-transport properties of thin granular Au/Al_2O_3 films in the vicinity of the percolation threshold. The current-voltage characteristics are found to vary dramatically from one tip position to another over distances of the order of a few nanometers. These characteristics often exhibit interesting Coulomb-staircase structures having unusual variations in step widths and heights due to complex tunneling paths. A triple-barrier tunnel-junction model accounts quantitatively for the experimental results.

Recent advances in transport measurements of mesoscopic tunnel junctions have succeeded in pushing the state of the art to the ultimate quantum limit. The quantized nature of the electrical charge significantly influences the electrical transport in such systems if the electrostatic charging energy involved in tunneling exceeds the thermal energy k_BT. This leads to single-electron tunneling (SET) effects such as the Coulomb blockade and Coulomb staircase.[1–7] The former manifests itself in the tunneling current-voltage (I-V) characteristics by the suppression of the current around zero bias voltage, while the latter exhibits a sequence of steps in the I-V curve. In the past few years the problem of SET was studied mainly for the double-barrier tunnel-junction (DBTJ) geometry, where a small metallic island is coupled via two tunnel junctions to two macroscopic electrodes.[1–7] The signature of SET, however, is also evident in much more complicated systems, such as granular metals. Granular metals are composite materials of small metal particles dispersed in a dielectric continuum.[8] Many of their intriguing electrical transport properties derive from single-electron tunneling between grains.[8,9] In all transport measurements done so far on these materials, the conductance properties result from an averaging over many conductance paths, each involving many tunneling events. The advent of scanning tunneling microscopy (STM) now provides the tool to observe transport properties locally.

In this paper we provide evidence that our understanding of mesoscopic systems of tunnel junctions may be extended by cryogenic STM studies of thin granular metal films. Disordered configurations of mesoscopic tunnel junctions are realized by the STM tip situated at different lateral positions along the film. Two aspects are being presented. First, we find strong fluctuations in the tunneling transport properties from one tip position to another, consistent with expectations for mesoscopic systems.[6,10] More important, our tunneling I-V characteristics frequently show interesting Coulomb-staircase structures, having steps with variable widths and heights. Such features were not observed previously for DBTJ, where the steps are *always* found to be of uniform height and *equidistantly* spaced, each step corresponding to the addition of a single electron onto the metallic island.[1–4,6] We can account quantitatively for our I-V characteristics in terms of a triple-barrier tunnel-junction (TBTJ) model, where the electron tunnels onto *two* small metallic particles along its path.

Our experimental setup consists of a cryogenic STM with a platinum-iridium tip, tunneling into a granular Au/Al_2O_3 film deposited by cosputtering gold and aluminum oxide onto a gold substrate. The films were ~ 15 nm thick, and the gold volume fractions were in the range of $0.3<x<0.45$, near and below the percolation threshold[8] which we measured to be around $x=0.4$. Under these conditions there are no more than 2–3 isolated Au particles spaced above each other across the film. Due to the exponential dependence of the tunneling current on distance, a dominant tunneling path is expected for each position of the tip over the granular film. An illustration of a dominant tunneling path along a TBTJ and the equivalent electrical circuit for this path are shown in Fig. 1, and will be discussed below.

The rapid variations of the local electrical transport prop-

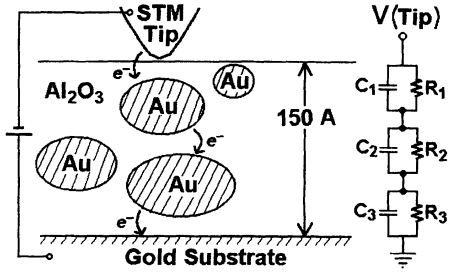

FIG. 1. A schematic of the experimental setup; a granular Au/Al_2O_3 film sandwiched between a STM tip and a metal substrate. A tunneling path across a triple-barrier tunnel junction is indicated by arrows. The equivalent electrical circuit is shown to the right.

0163-1829/94/50(12)/8961(4)/$06.00

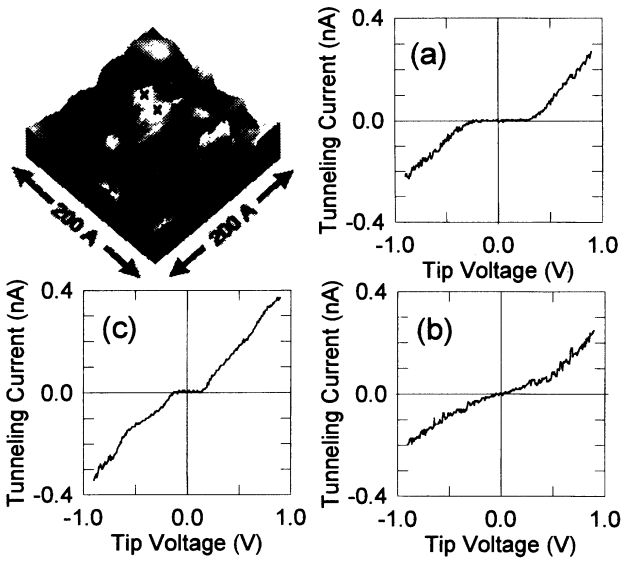

FIG. 2. A topographic image and three tunneling I-V characteristics of a Au/Al_2O_3 film of 30% Au volume percent at 78 K. The tip positions at which the curves were measured are indicated on the topographic image.

erties of granular metal films is demonstrated by Fig. 2. Here we present three tunneling I-V characteristics measured perpendicular to a granular Au/Al_2O_3 film at 78 K at different positions along the film. The gold volume fraction of the film was 0.3 (below the percolation threshold). The different positions are indicated on the STM topographic image, taken simultaneously with the I-V traces. The topographic image was taken in the constant-current mode with a reference current set at 0.5 nA and a tip bias of 1 V. The three I-V curves show qualitatively different behaviors: Curve (b) is purely metallic, while curves (a) and (c) exhibit Coulomb blockade. Curve (c) displays, in addition, also a weak Coulomb-staircase structure. The sensitivity to position of the local electrical transport properties is strikingly demonstrated by curves (a) and (b), taken at a lateral distance of only ~ 5 nm apart. The metallic curve (b) was probably taken with the tip situated above a large gold cluster connected to the metal substrate (although *globally* the sample was below the percolation threshold). Curve (a), on the other hand, shows a pronounced Coulomb blockade with a threshold voltage $V_t \simeq 0.3$ V, consistent with a DBTJ geometry. For a rough estimate we equate eV_t with the charging energy $e^2/2C$ and obtain a grain-to-environment capacitance C of around 2.5×10^{-19} F. This DBTJ is consistent with an $\sim$2-nm-diameter gold grain sandwiched in between the STM tip and the large gold cluster. It is interesting to note that while the I-V characteristics vary dramatically with lateral distance, the apparent topography does not reflect these variations. That is because with a tip bias much larger than V_t the contrast mechanism in the topographic mode is not very sensitive to fluctuations of the metal-insulator composition in the vicinity of the percolation threshold. We want to point out here that the energy gap of Al_2O_3 is well above 1 eV; thus curve (a) cannot reflect the density of states of the insulator. Indeed, we were not able to obtain STM images with a tip bias of 1 V for granular Au/Al_2O_3 films with $x<0.3$ because

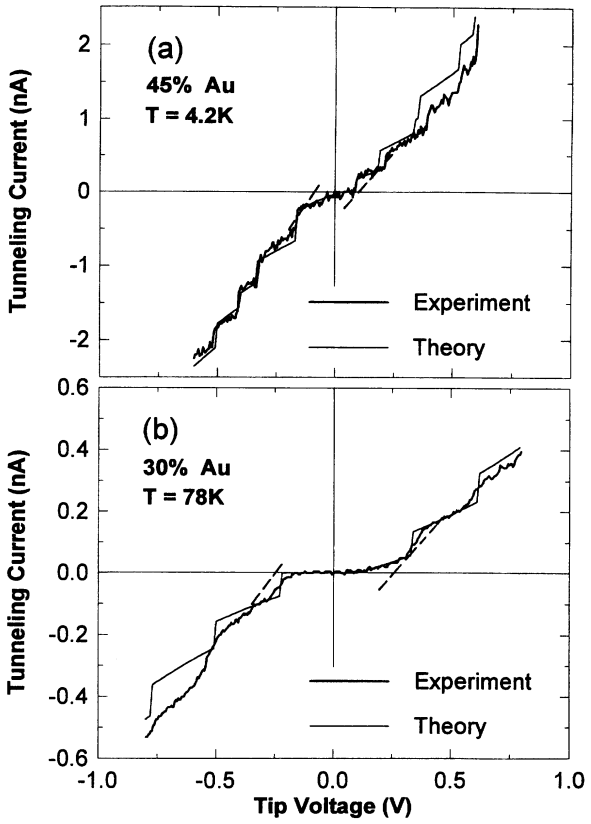

FIG. 3. Experimental tunneling I-V curves (heavy lines) with the corresponding theoretical curves (thin lines) calculated from our model. The dashed lines are the linear asymptotes to the experimental curves at large voltages.

the typical distance between gold particles becomes so large that tunneling is not observable.

In Fig. 3 we present two tunneling I-V characteristics showing Coulomb-staircase structures. The experimental curve (heavy line) in Fig. 3(a) was measured at 4.2 K on a film having a gold volume fraction of 0.45. The thin line is a theoretical curve calculated from our model, as discussed below. At first sight, the experimental curve shows a usual Coulomb-staircase structure similar to those observed for many DBTJ systems.[2–7] There are, however, three features in this tunneling I-V trace which are not consistent with a DBTJ geometry and were not reported previously. First, the steps are not equidistantly spaced; they have different widths ranging from 75 to 180 mV. Second, the steps are significantly narrower than the width of the region around zero bias between the positive and negative onsets of the Coulomb staircase, $\sim$245 mV. Most of the steps are narrower even than the displacement of $\sim$170 mV between the linear asymptotes (dashed lines) to the curve at large negative and positive voltages. Third, the current steps have different heights, ranging from 0.2 to 0.4 nA. These features appear in many of our I-V characteristics. However, we did obtain also I-V traces which conform closely to those expected[1–4] for strongly asymmetric DBTJ.

In order to account for the variable step-size Coulomb-staircase structures we assume that the dominant electron tunneling path consists of a triple-barrier tunnel junction, in-

volving electrons tunneling onto two metal grains, as shown in Fig. 1. Each junction $i=1,2,3$ is characterized by a tunneling resistance R_i and a capacitance C_i, as indicated in the schematic electrical circuit in the figure. The "state" of the system is determined by the number of excess electrons n_k on each grain $k=1,2$ which, in turn, depends on the applied voltage V. Our analysis is based on the "orthodox" theory[1-3] for SET and will be done here, for simplicity, for zero temperature.

In calculating the I-V characteristics of a TBTJ, one must first express the electron tunneling rates across each of the three junctions for a given state (n_1,n_2). Each rate depends on the tunneling resistance of the junction and the *total* energy change of the system due to the tunneling event. The electron tunneling rate on (+) or off (−) grain k across junction i is given at $T=0$ by[1,2]

$$\Gamma_{k,i}(n_1,n_2)^{\pm}=-\Delta E_{k,i}(n_1,n_2)^{\pm}/e^2R_i \tag{1}$$

for $\Delta E_{k,i}(n_1,n_2)^{\pm}\leq 0$ and 0 otherwise, where $\Delta E_{k,i}(n_1,n_2)^{\pm}$ is the energy change of the system due to the tunneling event. This energy depends, in general, on the number of excess electrons on *both* grains. There are two contributions to this energy, the change in the electrostatic charging energy of the system $\Delta U_{k,i}(n_1,n_2)^{\pm}$ and the potential difference V_i across the junction times the charge of the electron,

$$\Delta E^{\pm}_{k,i}=\Delta U^{\pm}_{k,i}\mp eV_i. \tag{2}$$

For brevity, in Eq. (2) and in what follows, the dependence of the energies on n_k is not indicated explicitly. V_i is easily expressed in terms of the applied voltage V and the TBTJ capacitances, for example, $V_3=C_1C_2V/\Sigma$, where $\Sigma=C_1C_2+C_1C_3+C_2C_3$. From Eqs. (1) and (2) one can see that at $T=0$ tunneling through a junction is blocked if the potential drop on that junction is too small to overcome the change in the charging energy. The charging energies $\Delta U^{\pm}_{k,i}$ are expressed in terms of the changes in the electrostatic charging energy of the individual grains, $\Delta U^{\pm}_k$:

$$\begin{aligned}\Delta U^{\pm}_1&=(C_3+C_2)\{(Q_1\pm e)^2-Q_1^2\}/2\Sigma,\\ \Delta U^{\pm}_2&=(C_1+C_2)\{(Q_2\pm e)^2-Q_2^2\}/2\Sigma,\end{aligned} \tag{3}$$

where $Q_k=n_ke-Q_{0k}$ is the excess charge on grain k before electron tunneling and Q_{0k} is the "residual fractional electron charge,"[1,2-6] $|Q_{0k}|\leq e/2$. When the electron tunnels through junctions 1 or 3, only one of the grains is charged, $\Delta U^{\pm}_{1,1}=\Delta U^{\pm}_1$ and $\Delta U^{\pm}_{2,3}=\Delta U^{\pm}_2$, while when the electron tunnels through junction 2 (from one grain to another), $\Delta U^{\pm}_{1,2}=\Delta U^{\pm}_{2,2}=\Delta U^{\pm}_1+\Delta U^{\mp}_2$. The expressions for the $\Delta E^{\pm}_{k,i}$ can now be written down explicitly,

$$\begin{aligned}\Delta E^{\pm}_{1,1}&=\{e/2\pm(n_1e-Q_{01})\mp VC_2C_3/(C_2+C_3)\}\\ &\quad\times e(C_2+C_3)/\Sigma,\\ \Delta E^{\pm}_{1,2}&=\{(C_1+2C_2+C_3)e/2\mp(C_1+C_2)(n_2e-Q_{02})\\ &\quad\pm(C_2+C_3)(n_1e-Q_{01})\pm VC_1C_3\}e/\Sigma,\end{aligned} \tag{4}$$

and similarly for $\Delta E^{\pm}_{2,2}$ and $\Delta E^{\pm}_{2,3}$.

The zero-temperature electron-tunneling rates $\Gamma_{k,i}(n_1,n_2)^{\pm}$ can now be calculated from Eqs. (1)–(4). From these one should first calculate the distribution $P(n_1,n_2)$ of the number of excess electrons on the grains as a function of the applied voltage.[1,2] At zero temperature, however, $P(n_1,n_2)$ is sharply peaked for each voltage around a most probable state (n_{01},n_{02}), thus the number of excess electrons on each grain is well defined for a given voltage. The n_{0k} are determined from the condition that the *total* tunneling rate on (off) each grain is smaller than the total tunneling rate on (off) the grain being in the state $n_{0k}-1$ $(n_{0k}+1)$. The tunneling current can now be calculated for any given junction:

$$I(V)=e\{\Gamma_{k,i}(n_{01},n_{02})^{+}-\Gamma_{k,i}(n_{01},n_{02})^{-}\}. \tag{5}$$

Similar to the case of DBTJ, we find that there is a discontinuous jump in the tunneling I-V characteristics each time n_{01} and/or n_{02} change their values. However, there is an important difference between the two cases. In the asymmetric DBTJ geometry the number of excess electrons on the center island is a periodic function of V, thus one expects to find *equidistantly* spaced steps in the Coulomb staircase, as indeed found experimentally.[2,5,6] In the TBTJ case, on the other hand, n_{01} and n_{02} are not necessarily periodic in V, and even in the case where each one in itself is periodic the two periods may differ. This will result in Coulomb-staircase structures having steps of different widths. The height of the steps may also vary, since the effect on the tunneling current due to a change in n_{01} may differ from that due to changing n_{02}.

Fitting our model to the experimental results for the most general TBTJ is very complicated, even in the zero-temperature limit. The fitting becomes simpler when assuming that the tunneling rate between the two grains, across junction 2, is much slower than the tunneling rates across the two outer junctions. This assumption is reasonable since the former process involves the charging of two grains, while the latter involves only one. Moreover, due to the geometry, fewer effective electron tunneling channels are available between two grains than between the tip or the substrate to a grain. In this case, n_{01} and n_{02} are determined independently by junctions 1 and 3 (i.e., by $\Gamma_{1,1}$ and $\Gamma_{2,3}$), respectively, and the current is then calculated using Eq. (5) for junction 2 (from $\Gamma_{1,2}$ or $\Gamma_{2,2}$). Our model accounts well for the experimental results even in this simplified form.

A theoretical I-V curve calculated from our TBTJ model at zero temperature and fitted to our experimental data, measured at 4.2 K, is shown in Fig. 3(a). The fitting parameters were $C_1=12\times10^{-19}$ F, $C_2=14\times10^{-19}$ F, $C_3=28\times10^{-19}$ F, and $R_2=280$ MΩ. The fit is indeed very good, considering the complexity of the TBTJ system at hand. Most of the features present in the experimental curve, both in the Coulomb-blockade region and the staircase structure, are reproduced quite accurately by the theoretical curve. We have followed a common procedure used in STM studies of DBTJ (Refs. 2,4–7) and took also I-V traces at the same lateral position but with a different tip-to-sample separation. Good fits to these traces were obtained by changing *only* the values of C_1 and the residual charges Q_{0k}, leaving the two other

(internal) junction parameters unchanged. This verifies the reliability of our model and the numbers obtained by the fits.

The experimental I-V trace (heavy line) shown in Fig. 3(b) was taken at 78 K, for the same Au/Al_2O_3 film as in Fig. 2, but at a different tip position. The Coulomb-staircase steps are not as sharp as those observed at 4.2 K, partly due to thermal effects.[1,2] Because of their large width only four steps are present within the voltage range at which the curve was measured. Yet, it is evident that this curve also displays features which are not consistent with a DBTJ structure. The steps (according to the four measured) seem to have nearly the same width, ~ 260 mV, but this width is much smaller than the region ~ 530 mV between the positive and negative onsets of the Coulomb staircase and the displacement of ~ 480 mV between the linear asymptotes (dashed lines) to the trace at large voltages. The theoretical curve (thin line) was again calculated from our model, taking $C_1 = C_3 = 8 \times 10^{-19}$ F, $C_2 = 4.5 \times 10^{-19}$ F, and $R_2 = 1.2$ GΩ. It reproduces correctly the onset of each step as well as the behavior around zero voltage before the onsets of the Coulomb staircase. It does not reproduce, however, the rounding in the steps and the slopes of the jumps. These two discrepancies nearly vanish in the full, finite-temperature calculations of our model, presented and discussed elsewhere.[11]

In conclusion, Coulomb-staircase structures were found in tunneling I-V characteristics of disordered arrays of mesoscopic tunnel junctions. The Coulomb-staircase data show features which are inconsistent with the DBTJ model, but are well accounted for by a triple-barrier tunnel-junction model developed by us. We have also demonstrated that cryogenic STM is an effective tool for studying the low-temperature local transport properties of granular metal films. The local transport properties are found to vary dramatically over distances of the order of a few nanometers. Future STM studies of granular metal films may reveal new SET phenomena and shed more light on the long-standing problem of the conductance mechanism in granular systems.[8,9,12]

We thank J. I. Gersten of the City College of the City University of New York for many helpful discussions, and M. Wolovelsky and D. Porath for their help in building the cryogenic STM.

---

*Author to whom correspondence should be addressed.

[1] D. V. Averin and K. K. Likharev, in *Mesoscopic Phenomena in Solids*, edited by B. L. Altshuler, P. A. Lee, and R. A. Webb (Elsevier, Amsterdam, 1991), p. 173.

[2] A. E. Hanna and M. Tinkham, Phys. Rev. B **43**, 5919 (1991).

[3] R. Wilkins, M. Amman, E. Ben-Jacob, and R. C. Jaklevic, J. Vac. Sci. Technol. B **9**, 996 (1992).

[4] C. Schonenberg, H. van Houten, and H. C. Donkersloot, Europhys. Lett. **20**, 249 (1992).

[5] Z. Y. Rong, A. Chang, L. F. Cohen, and E. L. Wolf, IEEE Trans. Magn. **28**, 67 (1992).

[6] J. G. A. Dubois, E. N. G. Verhijen, J. W. Gerritsen, and H. van Kempen, Phys. Rev. B **48**, 11 260 (1993).

[7] M. Amman, S. B. Field, and R. C. Jaklevic, Phys. Rev. B **48**, 12 104 (1993).

[8] B. Abeles, P. Sheng, M. D. Coutes, and Y. Arie, Adv. Phys. **24**, 407 (1975).

[9] *Physical Phenomena in Granular Materials*, edited by G. D. Cody, T. H. Geballe, and P. Sheng, MRS Symposia Proceedings No. 195 (Materials Research Society, San Francisco, 1990).

[10] P. A. Lee, D. A. Stone, and H. Fukuyama, Phys. Rev. B **35**, 1039 (1987).

[11] E. Bar-Sadeh *et al.*, J. Vac. Sci. Technol. (to be published).

[12] S. T. Chui, Phys. Rev. B **43**, 14 247 (1991).

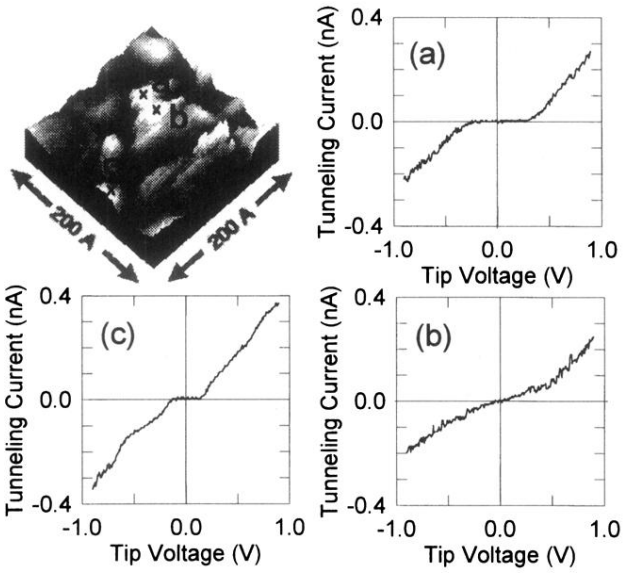

FIG. 2. A topographic image and three tunneling I-V characteristics of a Au/Al_2O_3 film of 30% Au volume percent at 78 K. The tip positions at which the curves were measured are indicated on the topographic image.